ORGANIC LETTERS

2013
Vol. 15, No. 15
4022–4025

A Ratiometric Near-Infrared Fluorescent Probe for Hydrazine and Its *in Vivo* Applications

Chong Hu, Wen Sun, Jianfang Cao, Pan Gao, Jingyun Wang, Jiangli Fan, Fengling Song, Shiguo Sun, and Xiaojun Peng*

State Key Laboratory of Fine Chemicals, Dalian University of Technology, No. 2 Linggong Road, High-tech District, Dalian 116024, P. R. China

pengxj@dlut.edu.cn

Received July 1, 2013

ABSTRACT

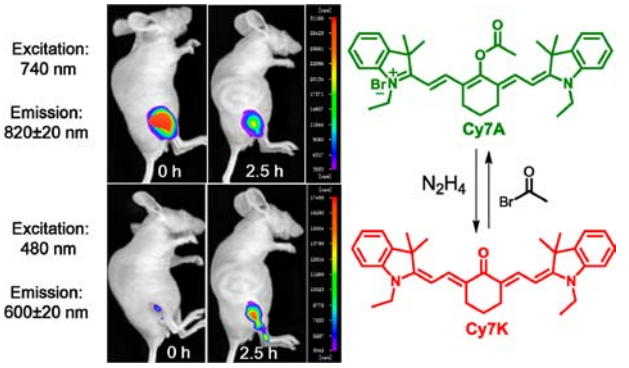

Based on modulation of the conjugated polymethine π-electron system of a cyanine dye derivative, a ratiometric near-infared fluorescent probe (Cy7A) for hydrazine (N_2H_4) has been designed and synthesized. Cy7A can be selectively hydrazinolysized with great changes in its fluorescent excitation/emission profiles, which makes it possible to detect N_2H_4 in water samples and living cells and, for the first time, visualize N_2H_4 in living mice.

Hydrazine (N_2H_4), a well-known high-energy propellant, is widely used in rocket-propulsion systems for its flammable and detonable characteristics.[1] Its reductibility and alkalinity also make it popular in many other industrial applications including metal anticorrosion, acting as a common precursor in the synthesis of various polymers, textile dyes, and pharmaceutical intermediates.[2] However, hydrazine is highly poisonous when inhaled or in contact with skin.[3] It has been reported that hydrazine is a neurotoxin and has severe mutagenic effects causing serious damage to the liver, lungs, kidneys, and the human central nervous system.[4] The U.S. Environmental Protection Agency (EPA) has classified hydrazine as a potential human carcinogen and recommended the threshold limit value (TLV) of hydrazine to be as low as 10 ppb.[1b] Therefore, reliable analytical approaches for hydrazine detection with satisfactory sensitivity and selectivity are of great interest and importance.

The traditional analytical techniques for the detection of hydrazine include coulometry,[5] potentiometry,[6] titration,[7] and colorimetry.[8] But they are always complex and time-consuming and/or need special equipment.[1a] Besides, they

(1) (a) Mo, J.-W.; Ogorevc, B.; Zhang, X.; Pihlar, B. *Electroanalysis* **2000**, *12*, 48–54. (b) Zelnick, S. D.; Mattie, D. R.; Stepaniak, P. C. *Aviat. Space Environ. Med.* **2003**, *74*, 1285–1291.

(2) (a) Hydrazine and Its Derivatives. In *Kirk-Othmer Encyclopedia of Chemical Technology*, 5th ed.; Kroschwitz, J. I., Seidel, A., Eds.; Wiley: NewYork, 2005; Vol. 13, pp 562−607. (b) Ragnarsson, U. *Chem. Soc. Rev.* **2001**, *30*, 205–213.

(3) (a) Reilly, C. A.; Aust, S. D. *Chem. Res. Toxicol.* **1997**, *10*, 328–334. (b) Garrod, S.; Bollard, M. E.; Nicholls, A. W.; Connor, S. C.; Connelly, J.; Nicholson, J. K.; Holmes, E. *Chem. Res. Toxicol.* **2005**, *18*, 115–122.

(4) International Agency for Research on Cancer: Re-evaluation of some organic chemicals, hydrazine, and hydrogen peroxide. IARC monographs on the evaluation of carcinogenic risk of chemicals to humans. Lyon, IARC, 1999, Vol. 71, pp 991−1013. http://monographs.iarc.fr/ENG/Monographs/vol71/mono71-43.pdf.

(5) Olson, E. C. *Anal. Chem.* **1960**, *32*, 1545–1547.

(6) Stetter, J. R.; Blurton, K. F.; Valentine, A. M.; Tellefsen, K. A. *J. Electrochem. Soc.* **1978**, *125*, 1804–1807.

(7) Malone, H. E. *Anal. Chem.* **1961**, *33*, 575–577.

(8) El-Brashy, A.; El-Hussein, L. *Synth. React. Inorg. Met.-Org. Chem.* **1997**, *30*, 609–622.

10.1021/ol401838p
Published on Web 07/22/2013

Scheme 1. Synthesis of **Cy7A** and the Proposed Recognition Mechanism of **Cy7A** toward Hydrazine in a Ratiometric Manner

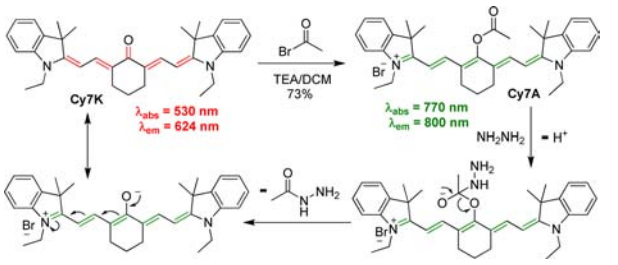

are not suitable for analyzing hydrazine *in vivo*, as they require post-mortem processing and destruction of tissues or cell lysates.[9] Recently, a fluorescent probe-based assay has gained increasing attention because of its high sensitivity and selectivity, simplicity for implementation, economy, real-time detection, noninvasiveness, and good compatibility for biosamples.[10] Compared to light in the ultraviolet/visible (UV/vis) region, near-infared light is much more favorable for biological imaging due to its minimum photodamage to biological samples, good tissue penetration, and weak autofluorescence interference from the complicated living systems.[11] On the other hand, fluorescence intensity-based measurements are sometimes problematic for accurate fluorometric analyses. In intricate biosystems, fluorescence intensity-based measurements are also influenced by the probe concentration, autofluorescence, or instrumental factors, which are disadvantageous to quantitative detection.[12] By contrast, a ratiometric approach can eliminate the effects of these factors to realize reliable quantitative detection by measuring the ratio of fluorescence intensities at two different wavelengths, thus arousing more attention.[13]

So far, abundant fluorescent probes for various analytes have been developed.[14] However, to date, small-molecule fluorescent probes for hydrazine detection are still very limited.[12,15] We recently reported a ratiometric

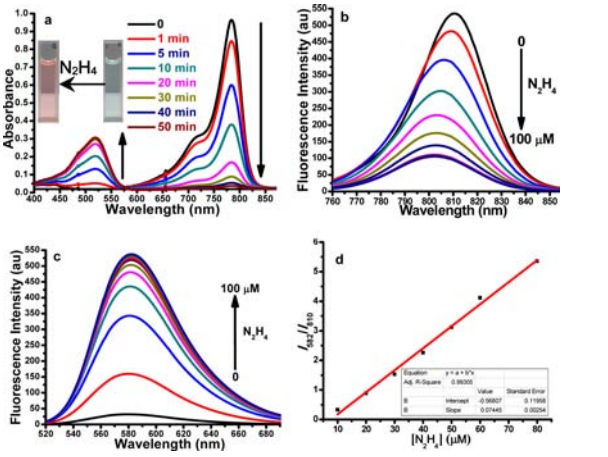

Figure 1. Absorption (a) and emission (b, c, d) spectra of **Cy7A** (5 μM) toward N_2H_4 in a mixture of acetate buffer (pH 4.5, 10 mM) and DMSO (1/9, v/v) at rt. (a) The absorption spectra of **Cy7A** after incubation with 20 equiv of N_2H_4 for 0, 1, 5, 10, 20, 30, 40, and 50 min, respectively. Inset: the color change before and after the reaction of **Cy7A** with N_2H_4. (b, c) Fluorescence spectra of **Cy7A** upon addition of increasing concentrations of N_2H_4 (0, 10, 20, 30, 40, 50, 60, 70, 80, 90, and 100 μM) when excited at 750 nm (b) and 510 nm (c), respectively. (d) The fluorescence intensity ratios of **Cy7A** were linearly related to the concentrations of hydrazine (10−80 μM). Linear regression equation: $I_{582}/I_{810} = -0.5681 + 0.07445 \times [N_2H_4](\mu M)$, $R^2 = 0.993$. For b, c, and d, each spectrum was obtained after the mixture was incubated for 40 min at rt.

hydrazine-selective probe based on a coumarin-like fluorophore.[12] However, there is still a blank in terms of a ratiometric fluorescent probe for hydrazine working in the near-infared region (NIR), and making hydrazine visable in living animals is a great challenge.

Herein, we present a new NIR ratiometric fluorescent probe **Cy7A** for hydrazine based on a heptamethine cyanine dye derivative because of its NIR excitation/emission, high extinction coefficient, low biological toxicity, good biocompatibility, and sufficient water solubility.[16] Our strategy to design **Cy7A** relies on modulating the conjugated polymethine π-electron system of the dye; for that, this strategy was demonstrated to be an efficient way to tune fluorescent excitation/emission profiles.[17] As a most reported recognition mechanism toward hydrazine, the selective deprotection of ester by hydrazine[15b−e] was also selected in our present work. We envisioned that, upon addition of hydrazine, the acetate moiety of **Cy7A** would be selectively hydrazinolysized to leave the enol form of **Cy7K**, which further underwent tautomerism to give its corresponding ketone form. Consequently, the different spectra characteristics of these two compounds make it possible for **Cy7A** to be a NIR ratiometric fluorescent probe for hydrazine.

(9) Yu, F.; Li, P.; Song, P.; Wang, B.; Zhao, J.; Han, K. *Chem. Commun.* **2012**, *48*, 2852–2854.

(10) (a) Zhang, J. F.; Zhou, Y.; Yoon, J.; Kim, J. S. *Chem. Soc. Rev.* **2011**, *40*, 3416–3429. (b) Chen, X.; Tian, X.; Shin, I.; Yoon, J. *Chem. Soc. Rev.* **2011**, *40*, 4783–4804.

(11) (a) Hilderbrand, S. A.; Weissleder, R. *Curr. Opin. Chem. Biol.* **2010**, *14*, 71–79. (b) Escobedo, J. O.; Rusin, O.; Lim, S.; Strongin, R. M. *Curr. Opin. Chem. Biol.* **2010**, *14*, 64–70.

(12) Fan, J.; Sun, W.; Hu, M.; Cao, J.; Cheng, G.; Dong, H.; Song, K.; Liu, Y.; Sun, S.; Peng, X. *Chem. Commun.* **2012**, *48*, 8117–8119.

(13) Peng, X.; Yang, Z.; Wang, J.; Fan, J.; He, Y.; Song, F.; Wang, B.; Sun, S.; Qu, J.; Qi, J.; Yan, M. *J. Am. Chem. Soc.* **2011**, *133*, 6626–6635.

(14) Some examples: (a) Yang, Y.; Zhao, Q.; Feng, W.; Li, F. *Chem. Rev.* **2012**, *113*, 192–270. (b) Fan, J.; Zhan, P.; Hu, M.; Sun, W.; Tang, J.; Wang, J.; Sun, S.; Song, F.; Peng, X. *Org. Lett.* **2013**, *15*, 492–495. (c) Yoo, J.; Yang, S. K.; Jeong, M.-Y.; Ahn, H. C.; Jeon, S.-J.; Cho, B. R. *Org. Lett.* **2003**, *5*, 645–648.

(15) (a) Chen, X.; Xiang, Y.; Li, Z.; Tong, A. *Anal. Chim. Acta* **2008**, *625*, 41–46. (b) Choi, M. G.; Hwang, J.; Moon, J. O.; Sung, J.; Chang, S.-K. *Org. Lett.* **2011**, *13*, 5260–5263. (c) Li, K.; Xu, H.-R.; Yu, K.-K.; Hou, J.-T.; Yu, X.-Q. *Anal. Methods* **2013**, *5*, 2653–2656. (d) Choi, M. G.; Moon, J. O.; Bae, J.; Lee, J. W.; Chang, S.-K. *Org. Biomol. Chem.* **2013**, *11*, 2961–2965. (e) Zhu, S.; Lin, W.; Yuan, L. *Anal. Methods* **2013**, *5*, 3450–3453.

(16) Xu, K.; Qiang, M.; Gao, W.; Su, R.; Li, N.; Gao, Y.; Xie, Y.; Kong, F.; Tang, B. *Chem. Sci.* **2013**, *4*, 1079–1086.

(17) (a) Guo, Z.; Nam, S.; Park, S.; Yoon, J. *Chem. Sci.* **2012**, *3*, 2760–2765. (b) Wang, X.; Sun, J.; Zhang, W.; Ma, X.; Lv, J.; Tang, B. *Chem. Sci.* **2013**, *4*, 2551–2556.

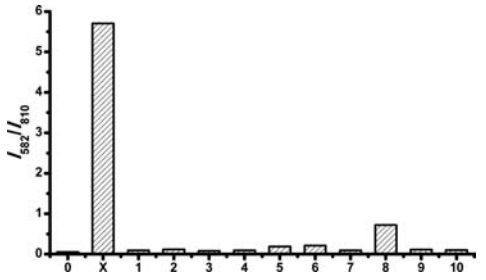

Figure 2. Fluorescence intensity ratios at 582 and 810 nm (I_{564}/I_{810}) of **Cy7A** (5 μM) upon the addition of N_2H_4 or other species (100 μM for N_2H_4, and 200 μM for the others). 0 blank, *X* N_2H_4, 1 cysteine, 2 lysine, 3 thiourea, 4 ammonia, 5 methylamine, 6 ethylenediamine, 7 urea, 8 hydroxylamine, 9 glutamine, 10 glutathione. Each spectrum was recorded after 40 min of reaction in a mixture of acetate buffer (pH 4.5, 10 mM) and DMSO (1/9, v/v) at rt.

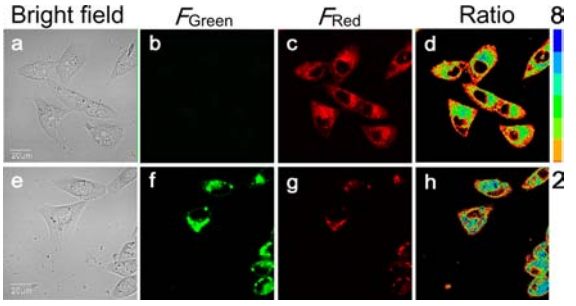

Figure 3. Confocal fluorescence images and fluorescence ratio (F_{Green}/F_{Red}) images of MCF-7 cells before (a, b, c, d) and after (e, f, g, h) loading the cells with N_2H_4. (a, b, c, d) Cells incubated with **Cy7A** (5 μM) for 0.5 h. (e, f, g, h) Cells incubated with **Cy7A** (5 μM) for 0.5 h and then treated with N_2H_4 (50 μM) for another 1 h. (a and e) Bright field images. (b and f) Green channel (pseudocolor, 575−620 nm), λ_{ex} = 559 nm. (c and g) Red channel (655−755 nm), λ_{ex} = 635 nm. (d and h) Fluorescence ratio (F_{Green}/F_{Red}) images. The ratiometric images were obtained by the image analysis software, Image Pro-plus 6.0. Scale bar: 20 μm.

As shown in Scheme 1, **Cy7A** was readily synthesized with a satisfactory yield (73%) and well characterized by ^{1}H NMR, ^{13}C NMR, and HRMS. The detailed synthetic procedures (Scheme S1) and the characterization spectra (Figures S15−S20) are described in the Supporting Information. Scheme 1 also depicts the possible ratiometric mechanism of **Cy7A** toward hydrazine.

With these two compounds in hand, we first investigated their absorption and emission spectra in methanol. As can be seen in Figure S1, **Cy7K** has maximum absorption and emission peaks at 530 and 624 nm (Φ_F = 0.340), respectively, while **Cy7A** has an absorption band of absorption maximum at 770 nm and an emission band at around 800 nm (Φ_F = 0.044). Apparently, there exist almost no overlaps in both absorption (Figure S1a) and emission (Figure S1b) spectra of **Cy7K** and **Cy7A**. This result ensures **Cy7A** to be a highly efficient ratiometric probe.

Subsequently, we elaborated the optical response of **Cy7A** to hydrazine in a mixture of acetate buffer (pH 4.5, 10 mM) and DMSO (1/9, v/v) at room temperature (rt). In the absence of hydrazine, the UV−vis spectra of **Cy7A** exhibited a maximum absorption at 784 nm ($\varepsilon = 1.9 \times 10^5$ M^{-1} cm^{-1}, Figure 1a). However, upon addition of hydrazine (20 equiv), the absorption at 784 nm decreased evidently, while a new flat absorption band of the absorption maximum at 520 nm ($\varepsilon = 6.1 \times 10^4$ M^{-1} cm^{-1}, Figure 1a) appeared gradually and then reached a plateau within about 40 min (Figures 1a and S2). Such a great hypsochromic shift of 264 nm in the absorption spectra changed the color of the solution from light green to red (inset of Figure 1a), allowing the colorimetric detection of hydrazine by the "naked eye". Consistently, with the increase of hydrazine concentration ([N_2H_4]) added (0−20 equiv), the emission at 810 nm (λ_{ex} = 750 nm) for **Cy7A** decreased distinctly (Figure 1b). By contrast, a new emission band centered at around 582 nm (λ_{ex} = 510 nm) arose and gradually enhanced in intensity with the increase of [N_2H_4] (Figure 1c). As a result, a large hypsochromic shift of 228 nm in the characteristic emission band was observed after the specific reaction between **Cy7A** and hydrazine. The corresponding product was verified to be **Cy7K** (Figures S6, S7, S21). In addition, the fluorescence intensity ratio at 582 and 810 nm (I_{810}/I_{582}) also increased with the increase of [N_2H_4] (Figure S3), and a linear relationship was observed between I_{810}/I_{582} and [N_2H_4] in the range of 10−80 μM (Figure 1d). Thus, the detection limit (3σ/slope) was calculated to be 2.5×10^{-8} M (0.81 ppb), which is essentially lower than that of TLV (10 ppb) according to the EPA. All the above results established that **Cy7A** could detect hydrazine both qualitatively and quantitatively.

Then we examined the specificity of **Cy7A** toward hydrazine. As shown in Figures S8 and S9, other cations represented by Na^+, K^+, Ca^{2+}, Mg^{2+}, Cd^{2+}, Pb^{2+}, Hg^{2+}, Zn^{2+}, Fe^{3+}, Fe^{2+}, Ag^+, Cu^{2+}, Co^{3+}, Ni^{2+}, Al^{3+}, and NH_4^+ as well as anions such as HPO_4^{2-}, ClO_4^-, CO_3^{2-}, ClO^-, Cl^-, I^-, BO_3^-, SO_4^{2-}, and NO_3^-, which were environmental and/or biological abundant, led almost to no changes to the absorption and emission spectra of **Cy7A**. Furthermore, **Cy7A** can respond to hydrazine well in the presence of these ions (Figures S10 and S11). The fluorescence ratio detection of hydrazine could also survive from the possible interference that arose from these ions (Figure S12). It is noteworthy that other compounds closely related to hydrazine such as hydroxylamine, ethylenediamine, ammonia, methylamine, urea, thiourea, and other common nucleophilic reagents led by cysteine, lysine, glutamine, and glutathione were also examined in our work (Figure 2). It was found that only hydroxylamine (40 equiv) could cause non-neglectable signal changes in the absorption (Figure S13) and emission (Figure S14) spectra of **Cy7A** in the test system, but the corresponding fluorescence intensity ratio (0.72) was still small (only about one-eighth of the value induced by hydrazine (5.7)), which will not pose a threat to the quantitative

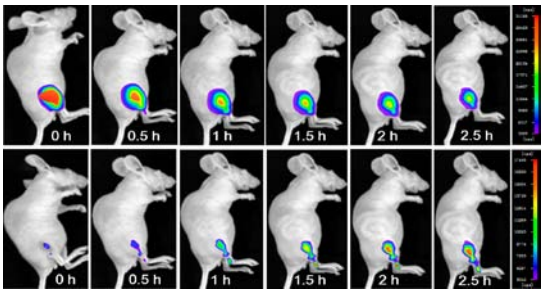

Figure 4. Representative fluorescence images (pseudocolor) of a nude mouse given a skin-pop injection of **Cy7A** (25 μL, 50 μM in a mixture of acetate buffer (pH 4.5, 10 mM) and DMSO (1/9, v/v)) and a subsequent skin-pop injection of N_2H_4 (25 μL, 500 μM in a mixture of acetate buffer (pH 4.5, 10 mM) and DMSO (1/9, v/v)). Images were taken after incubation for 0, 0.5, 1, 1.5, 2, and 2.5 h, respectively. The top images were taken with an excitation laser of 740 nm and an emission filter of 820 $\pm$ 20 nm, and the bottom ones were taken with an excitation laser of 480 nm and an emission filter of 600 $\pm$ 20 nm.

detection of hydrazine. So, it is corroborated that **Cy7A** can detect hydrazine with satisfactory selectivity.

In order to realize the value of **Cy7A**, we next studied the ability of **Cy7A** in practical applications. Prior to living cell imaging and living mice imaging, **Cy7A** was first subjected to hydrazine detection in two real water samples. The hydrazine concentrations detected by our method were found to be in good agreement with the amounts of hydrazine added (Table S1). The results make us believe that **Cy7A** would be qualified to detect hydrazine in real water samples quantitatively.

Then we investigated the potential of **Cy7A** for its *in vivo* applications. Confocal fluorescence imaging in living MCF-7 cells was carried out (Figure 3). MCF-7 cells incubated with **Cy7A** (5 μM) for 0.5 h showed strong red fluorescence at 655−755 nm, while the green fluorescence image (pseudo color) obtained at 575−620 nm was very weak, suggesting that **Cy7A** was living cell membrane permeable. By contrast, after the addition of hydrazine (50 μM) and then incubation for another 1 h, the fluorescence intensity in the green channel increased obviously and the red fluorescence diminished simultaneously. Combined with the fluorescence ratio images of living MCF-7 cells before (Figure 3d) and after (Figure 3h) the treatment of hydrazine, **Cy7A** was confirmed to be competent for imaging hydrazine in living cells in a ratiometric manner.

Being encouraged by the successful utilization of **Cy7A** in imaging hydrazine in living cells, we further evaluated the suitability of **Cy7A** for monitoring hydrazine in living animals. Nude mice were selected as our model and were given skin-pop injections of **Cy7A** and hydrazine in order, as the skin-pop-injection method will make it possible to detect hydrazine *in vivo* at the first stage, which is very significant and valuable to prevent the deeper damage triggered by hydrazine. As can be seen in Figure 4, after being incubated for a certain time, a representative nude mouse exhibited distinct fluorescence signal changes at two emission channels. The top images present a visible decrease in fluorescence intensity. In contrast, the bottom ones show apparent fluorescence enhancement. With the above results taken together, it was revealed that **Cy7A** could, for the first time, image hydrazine in living mice by monitoring the signal changes of two different fluorescence channels.

In summary, we have developed a selective ratiometric NIR fluorescent probe **Cy7A** for hydrazine based on modulation of the conjugated polymethine π-electron system of the dye. Upon addition of hydrazine, the fluorescent excitation and emission profiles of **Cy7A** changed significantly (from 784 to 520 nm in absorption spectra and from 810 to 582 nm in emission spectra). **Cy7A** showed a ratiometric fluorescence response that was selective for hydrazine over other species with a detection limit of 0.81 ppb. Moreover, it could be used to detect hydrazine in real water samples quantitatively, image hydrazine in living cells in a ratiometric manner, and, for the first time, visualize hydrazine in living mice by monitoring the signal changes of two different fluorescence channels.

Acknowledgment. This work was financially supported by the National Science Foundation of China (21136002, 21076032, and 20923006), the National Basic Research Program of China (2009CB724706 and 2012CB733702), and National High Technology Research and Development Program of China (863 program 2011AA02A105).

Supporting Information Available. Experimental details, characterization data of compounds, and additional spectroscopic data. This material is available free of charge via the Internet at http://pubs.acs.org.

The authors declare no competing financial interest.